Farnesoid X receptor is essential for normal glucose homeostasis

Ke Ma,[1] Pradip K. Saha,[2] Lawrence Chan,[2] and David D. Moore[1]

[1]Department of Molecular and Cellular Biology and [2]Section of Endocrinology and Metabolism, Departments of Molecular and Cellular Biology and Medicine, Baylor College of Medicine, Houston, Texas, USA.

The bile acid receptor farnesoid X receptor (FXR; NR1H4) is a central regulator of bile acid and lipid metabolism. We show here that FXR plays a key regulatory role in glucose homeostasis. FXR-null mice developed severe fatty liver and elevated circulating FFAs, which was associated with elevated serum glucose and impaired glucose and insulin tolerance. Their insulin resistance was confirmed by the hyperinsulinemic euglycemic clamp, which showed attenuated inhibition of hepatic glucose production by insulin and reduced peripheral glucose disposal. In *FXR*$^{-/-}$ skeletal muscle and liver, multiple steps in the insulin signaling pathway were markedly blunted. In skeletal muscle, which does not express FXR, triglyceride and FFA levels were increased, and we propose that their inhibitory effects account for insulin resistance in that tissue. In contrast to the results in *FXR*$^{-/-}$ mice, bile acid activation of FXR in WT mice repressed expression of gluconeogenic genes and decreased serum glucose. The absence of this repression in both *FXR*$^{-/-}$ and small heterodimer partner–null (*SHP*$^{-/-}$) mice demonstrated that the previously described FXR-SHP nuclear receptor cascade also targets glucose metabolism. Taken together, our results identify a link between lipid and glucose metabolism mediated by the FXR-SHP cascade.

Introduction

The farnesoid X receptor (FXR; NR1H4) is a member of the nuclear receptor superfamily that is primarily expressed in liver, kidney, and intestine. It forms a heterodimer with retinoid X receptor and binds inverted repeats of 2 AGGTCA half sites separated by 1 nucleotide, insulin receptor 1 (IR-1), to regulate target gene transcription. Bile acids are its endogenous ligands (1–3), and FXR plays an essential role in the feedback regulation of bile acid biosynthesis through repression of the key enzyme cholesterol-7α hydroxylase (CYP7A1) (4). FXR activation induces expression of the orphan nuclear receptor small heterodimer partner (SHP; NR0B2), which inhibits CYP7A1 gene expression by blocking the activity of another orphan receptor, the liver receptor homolog (LRH-1; NR5A2). Studies with *SHP*$^{-/-}$ mice confirmed the importance of this nuclear receptor pathway for negative regulation of bile acid synthesis and also revealed SHP-independent pathways (5–7).

FXR also plays an important role in lipoprotein metabolism. This was suggested by the identification of genes encoding phospholipid transfer protein (8), apoC-II, apoC-III, and apoA-I (9, 10) as FXR targets and confirmed by the demonstration of altered lipid metabolism in *FXR*$^{-/-}$ mice, which exhibit elevated plasma cholesterol and triglyceride levels and excessive accumulation of fat in the liver (11, 12). Fatty liver disease, or hepatic steatosis, is one of the most common liver diseases in humans (13) and is associated with defects in insulin action that are independent of overall body weight. Thus, type 2 diabetes patients with fatty liver are substantially more insulin resistant and have higher levels of plasma FFAs than those without it (14). However, the precise mechanisms linking fatty liver to diabetes are poorly understood.

Recent reports (15–19) have suggested potential involvement of FXR in glucose homeostasis. Several studies (15, 17, 18) indicate that bile acids alter expression of genes involved in gluconeogenesis, including phosphoenoylpyruvate kinase (PEPCK), glucose-6-phosphatase (G-6-Pase), and fructose-1,6-biphosphatase, although the mechanisms that mediate these responses remain unclear.

To explore the role of FXR in glucose homeostasis, we compared glucose metabolism in WT and *FXR*$^{-/-}$ mice. *FXR*$^{-/-}$ mice showed impaired glucose tolerance, decreased insulin sensitivity, and significantly blunted insulin responsiveness in both skeletal muscle and liver. On the other hand, activation of FXR by dietary cholic acid (CA) suppressed expression of multiple genes involved in gluconeogenesis and lowered glucose level. Both of these responses were lost in *FXR*$^{-/-}$ and *SHP*$^{-/-}$ mice. These results reveal that FXR is required for the maintenance of normal glucose metabolism and provide a specific molecular link between fatty liver and insulin resistance. *FXR*$^{-/-}$ mice provide what we believe to be a unique animal model for the role of fatty liver in the metabolic syndrome.

Results

Abnormal glucose metabolism in FXR$^{-/-}$ *mice*. Mice deficient in FXR display elevated plasma cholesterol and triglyceride levels due to the loss of FXR regulation of hepatic bile acid and lipid metabolism (12). In accord with previous results, we observed increased plasma cholesterol and triglyceride levels in *FXR*$^{-/-}$ mice (Figure 1, A and B). The *FXR*$^{-/-}$ mice also exhibited increased hepatic triglyceride accumulation (Figure 1D) accompanied by marked induction of several genes involved in lipogenesis, such as SREBP-1c, stearoyl-CoA desmutase, and fatty acid synthase (Figure 1E). In addition, the level of circulating FFAs was approximately 2-fold higher in the *FXR*$^{-/-}$ mice (Figure 1C). These elevated FFA levels were comparable to those of WT mice fed a high-fat diet for 3 months and were not further increased by feeding the *FXR*$^{-/-}$ mice a high-fat diet.

Due to the well-established role of high FFA levels in the pathogenesis of insulin resistance, we investigated glucose homeostasis in the *FXR*$^{-/-}$ mice. The serum glucose levels of random-fed

Nonstandard abbreviations used: CA, cholic acid; CYP7A1, cholesterol-7α hydroxylase; FXR, farnesoid X receptor; G-6-Pase, glucose-6-phosphatase; GTT, glucose tolerance test; IR, insulin receptor; IRS, insulin receptor substrate; ITT, insulin tolerance test; L-FABP, liver type FFA–binding protein; PEPCK, phosphoenoylpyruvate kinase; PGC-1α, PPARγ coactivator-1α; SHP, small heterodimer partner.

Conflict of interest: The authors have declared that no conflict of interest exists.

Citation for this article: *J. Clin. Invest.* **116**:1102–1109 (2006). doi:10.1172/JCI25604.

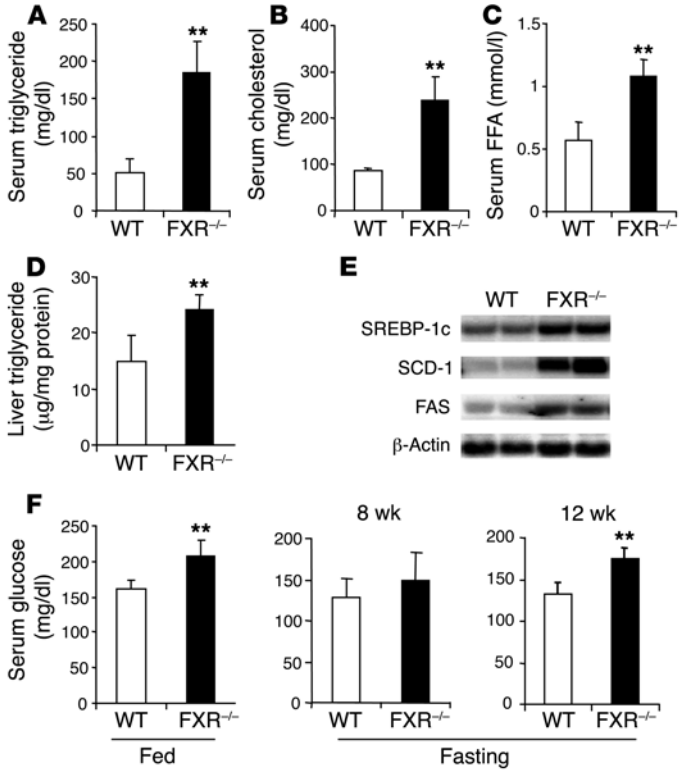

Figure 1
Lipid abnormalities in *FXR*$^{-/-}$ mice. Elevated plasma triglyceride (**A**), cholesterol (**B**), and FFA levels (**C**) were observed in *FXR*$^{-/-}$ mice compared with WT mice (n = 8–11 per group) after overnight fasting. (**D**) Elevated liver triglyceride content was seen in *FXR*$^{-/-}$ mice. (**E**) Induction of genes involved in lipogenesis in the liver in *FXR*$^{-/-}$ mice at random-fed state. RNA samples were pooled from 5 mice in each group and loaded in duplicates. FAS, fatty acid synthase; SCD-1, stearoyl-CoA desmutase 1. (**F**) Plasma glucose levels in random-fed and fasting states. $^{**}P < 0.01$ versus WT.

FXR$^{-/-}$ mice were approximately 30% higher than those of the WT mice, whereas fasting glucose levels showed an age-dependent increase, with significantly higher levels in 12-week-old mice (Figure 1F). In the glucose tolerance test (GTT), glucose levels were elevated at all time points after loading in the *FXR*$^{-/-}$ mice, reaching almost twice the WT levels at 2 hours (Figure 2A). The failure of the *FXR*$^{-/-}$ glucose levels to return to baseline suggests markedly impaired peripheral glucose uptake. Insulin levels during the GTT also deviated from the normal response in WT mice. The insulin response to glucose in *FXR*$^{-/-}$ mice was diminished, with levels persistently elevated at 2 hours when those of the WT had returned to baseline (Figure 2B). The insulin tolerance test (ITT) confirmed the impaired insulin sensitivity in *FXR*$^{-/-}$ mice (Figure 2C). Fifteen minutes after i.p. insulin challenge, WT glucose levels dropped to about 50% of baseline, while the *FXR*$^{-/-}$ levels decreased by only 23%. The *FXR*$^{-/-}$ mice also showed faster recovery to about 55% of baseline at 90 minutes, compared with 33% in the WT mice.

To examine the possible contribution of nonhepatic insulin sensitizing factors to the dysregulation of glucose metabolism in the *FXR*$^{-/-}$ mice, serum leptin and adiponectin were measured. The levels of these 2 major adipokines were comparable between *FXR*$^{-/-}$ and WT mice (data not shown).

The hyperinsulinemic euglycemic clamp was used to characterize glucose metabolic abnormalities in the absence of FXR in more detail. The contribution of liver glucose output to overall glucose metabolism was examined under both basal and low-dose insulin clamp conditions. *FXR*$^{-/-}$ and WT mice exhibited similar basal glucose production (Figure 3A) in the absence of insulin infusion. However, under the low-dose insulin clamp (3 U/kg/min), glucose output from the liver was completely suppressed in WT but not *FXR*$^{-/-}$ mice (Figure 3B). Note that the negative value of glucose production rate shown for WT mice was a result of the calculation used when the radioactive tracer was enriched instead of being diluted in plasma. In addition, the markedly lower rates for both glucose infusion and glucose disposal under low- and high-dose clamp conditions demonstrate a substantial defect in peripheral insulin sensitivity (Figure 3, C and D). Taken together, these data show that both failure of suppression of glucose production by the liver and attenuated peripheral disposal led to overall glucose intolerance in *FXR*$^{-/-}$ mice.

Impaired insulin signaling in FXR$^{-/-}$ *skeletal muscle and liver.* A major consequence of elevated circulating FFA is interference with the insulin signaling cascade, which could account for the peripheral insulin resistance. Thus we investigated insulin action in skeletal muscle of WT and *FXR*$^{-/-}$ mice. After insulin administration, IR tyrosine phosphorylation was attenuated in the *FXR*$^{-/-}$ muscle (Figure 4A), and the level of insulin receptor substrate–1 (IRS-1) associated with PI3K was also markedly decreased (Figure 4B). Insulin-stimulated PI3K activity, measured in anti-phosphotyrosine antibody IPs from muscle homogenates of *FXR*$^{-/-}$ mice, was decreased to approximately 50% that of WT mice (Figure 4C). Similarly, insulin failed to stimulate serine phosphorylation of the Akt kinase in *FXR*$^{-/-}$ mice, though it led to a robust response in WT mice (Figure 4D). The higher basal activation of Akt in the absence of FXR could be the result of the

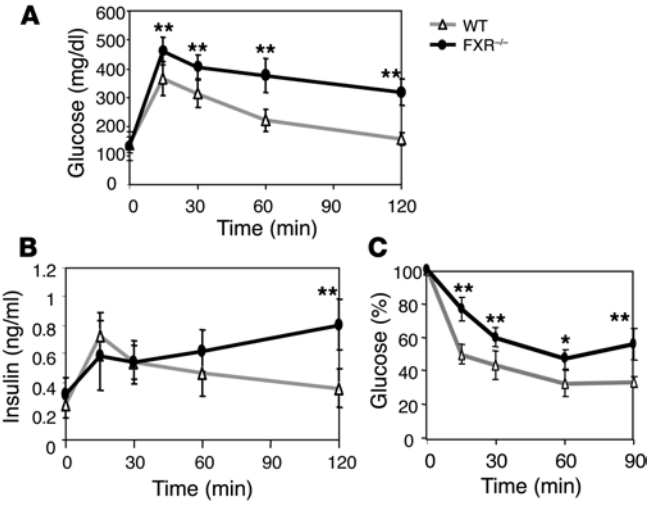

Figure 2
Impaired insulin sensitivity in *FXR*$^{-/-}$ mice. Glucose (**A**) and insulin (**B**) levels during 2 g/kg i.p. GTT in 8-week-old mice (n = 8–10 per group) after overnight fasting. (**C**) Glucose level during i.p. ITT in the fed state (n = 8–10 mice per group). $^{*}P < 0.05$, $^{**}P < 0.01$ versus WT.

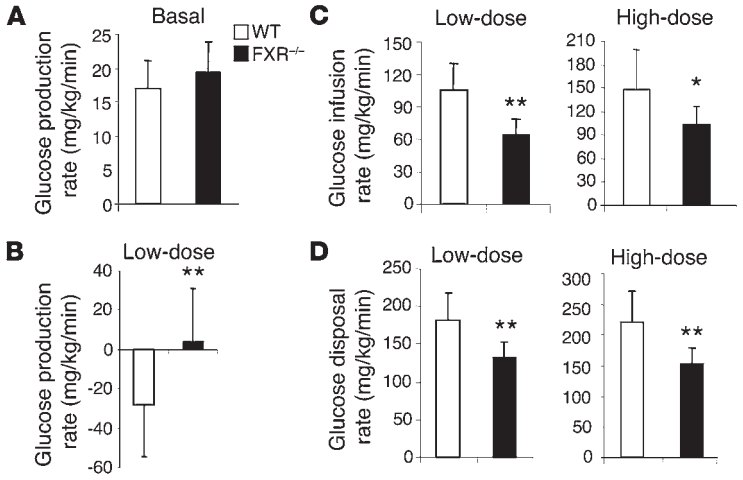

Figure 3
Low-dose and high-dose hyperinsulinemic-euglycemic clamp in 8- to 10-week-old WT and *FXR*$^{-/-}$ mice (n = 6 per group). (**A** and **B**) Glucose production rate under basal (before insulin infusion; **A**) and low-dose clamp (3 mU/kg/min; **B**) conditions. (**C**) Glucose infusion rate during low- (3 mU/kg/min) and high-dose clamp (10 mU/kg/min) conditions. (**D**) Glucose disposal rate during low- and high-dose clamp conditions. *P < 0.05, **P < 0.01 versus WT.

elevated level of serum bile acid in these mice, which is known to activate both the JNK and MAPK pathways (20–22).

The effect on insulin signaling cannot be due to any direct consequences of loss of FXR function in skeletal muscle, since sensitive RT-PCR did not detect expression in that tissue (Figure 4E). Due to the well-documented inverse correlation between insulin sensitivity and the amount of intramuscular fat in skeletal muscle, we analyzed intramuscular triglyceride and FFA content, which were both markedly elevated in the *FXR*$^{-/-}$ tissue (Figure 4, F and G). Consistent with this, we observed an increased level of IRS-1 serine 307 phosphorylation (Figure 4H), which has previously been linked to triglyceride-induced insulin resistance (23). Interestingly, expression of several PPARα target genes involved in fatty acid metabolism, including the FFA transporter CD36 and the mitochondrial and peroxisomal oxidation enzymes acyl-CoA oxidase and long-chain fatty acid dehydrogenase, was induced in *FXR*$^{-/-}$ muscle (Figure 4I), suggesting that lipid accumulation and substantial defects in insulin signaling occur despite augmented FFA transport and oxidation.

The major effect of insulin in liver is suppression of gluconeogenesis. Since FXR deficiency led to defective insulin inhibition of hepatic glucose output (Figure 3B), the insulin response was examined in *FXR*$^{-/-}$ livers. Insulin-dependent IR phosphorylation (Figure 5A) and IRS-2 association with PI3K (Figure 5B) were markedly blunted, suggesting substantial insulin resistance. The basis

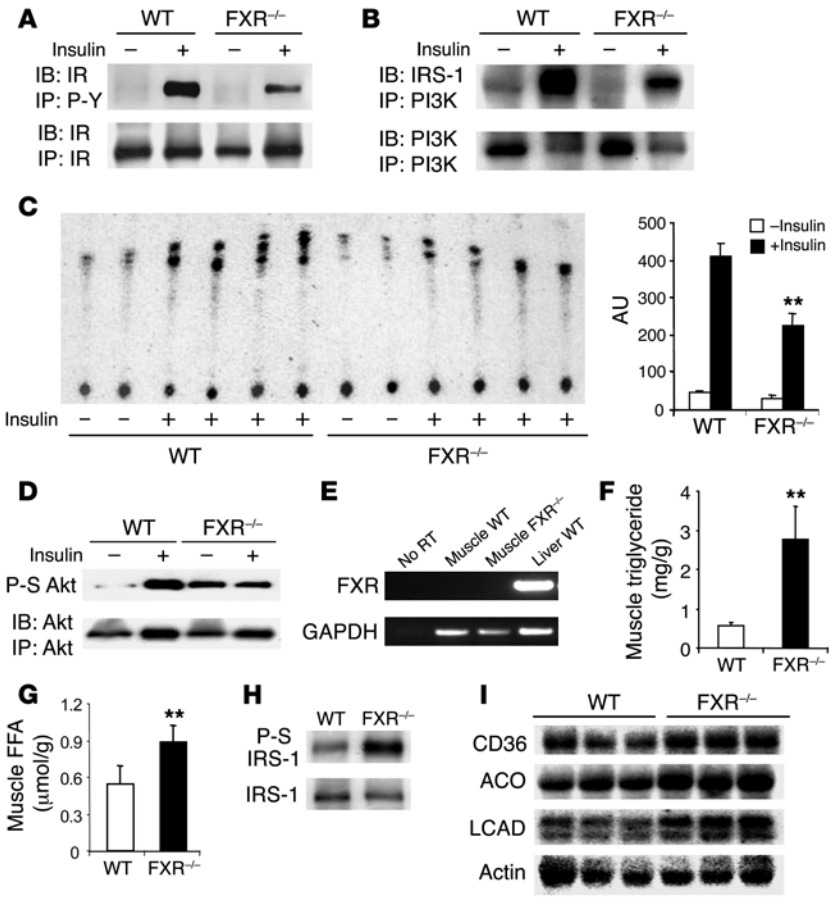

Figure 4
Impaired insulin signaling and upregulation of genes involved in fatty acid metabolism in muscle of *FXR*$^{-/-}$ mice. Muscle tissue homogenate from 4–5 mice per group were pooled together and subjected to IP and IB using antibodies as indicated. Northern blot analysis was performed on individual mice. Results are representative of at least 3 independent experiments. (**A**) Phosphorylation of IR after insulin stimulation (1 U/kg). Muscle homogenates were subjected to IP by anti-phosphotyrosine (P-Y) antibody 4G10 and IB by IR antibody. Total IR level was analyzed by IP followed by IB using the IR antibody. Quantitation was derived from 3 independent experiments. (**B**) Level of PI3K-associated IR after insulin stimulation as analyzed by IP using PI3K antibody followed by IRS-1 IB. (**C**) PI3K activity assay using immunopricipitates by anti-phosphotyrosine antibody. Muscle homogenates from individual mice were subjected to IP by anti-phosphotyrosine antibody followed by PI3K assay. Quantitation was derived from individual mice. (**D**) Phosphorylation of Akt (serine 473; P-S Akt) after insulin stimulation. (**E**) FXR expression by RT-PCR. (**F** and **G**) Analysis of intramuscular triglyceride and FFA content (n = 8 per group). (**H**) Serine 307 phosphorylation (P-S) of IRS-1 in the muscle after IP using IRS-1 antibody. (**I**) Expression of genes involved in fatty acid transport and oxidation in WT and *FXR*$^{-/-}$ muscle. ACO, acyl-CoA oxidase; LCAD, long-chain acyl-CoA dehydrogenase. **P < 0.01.

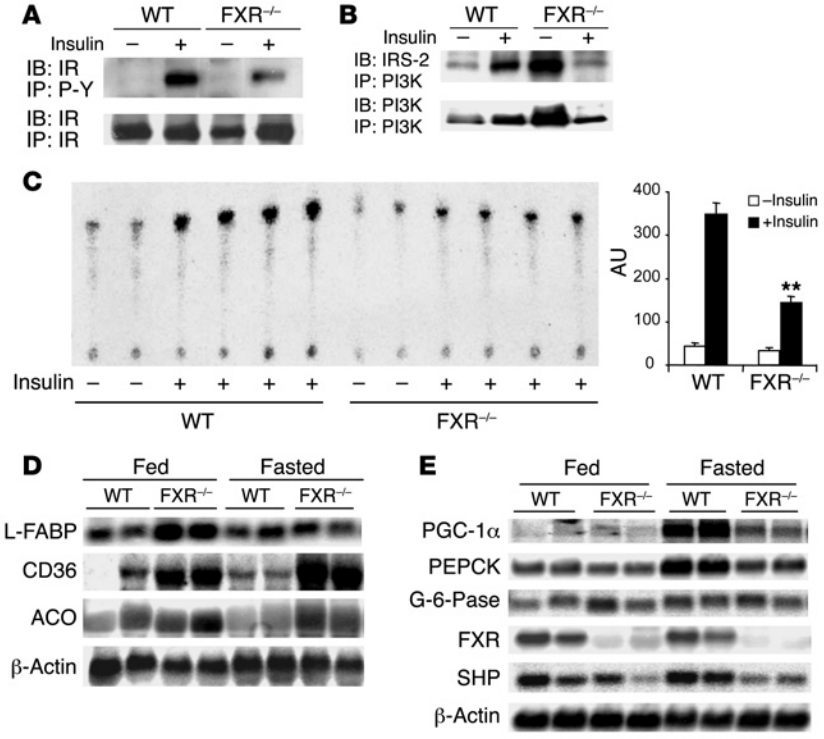

Figure 5
Impaired hepatic insulin signaling and expression of fatty acid metabolism and gluconeogenesis in the livers of *FXR*$^{-/-}$ mice. Liver tissue homogenates from 4–5 mice per group were pooled together and subjected to IP and IB using antibodies as indicated. Northern blot analysis was performed on individual mice. Results are representative of — and quantitation was derived from — at least 3 independent experiments. (**A**) Phosphorylation of IR after insulin stimulation (1U/kg). Liver homogenates were subjected to IP by anti-phosphotyrosine antibody 4G10 and IB by IR antibody. Total IR level was analyzed by IP followed by IB using the IR antibody. Quantitation was derived from 3 independent experiments. (**B**) PI3K-associated IRS-2 level. (**C**) PI3K activity assay using immunoprecipitates by anti-phosphotyrosine antibody. Liver homogenates from individual mice were subjected to IP by anti-phosphotyrosine antibody followed by PI3K assay. Quantitation was derived from individual mice. (**D**) Hepatic expression of genes involved in fatty acid transport and oxidation. L-FABP, liver type FFA–binding protein. (**E**) Hepatic expression of genes involved in gluconeogenesis. $^{**}P < 0.01$.

for the increased basal expression of IRS-2 and association with PI3K in untreated *FXR*$^{-/-}$ mice is unclear, but it could be secondary to elevated hepatic bile acid levels. Furthermore, insulin-induced PI3K activity in the *FXR*$^{-/-}$ livers was only approximately 30% that of WT mice in anti-phosphotyrosine antibody IPs (Figure 5C). As in the muscle, increased expression of PPARα target genes, including liver type FFA–binding protein, CD36, and acyl-CoA oxidase (Figure 5D), suggested increased FFA load. Interestingly — and in accord with a recent report (19) — the fasting response of key gluconeogenic factors, including PPARγ coactivator-1α (PGC-1α) and PEPCK, was diminished in the *FXR*$^{-/-}$ mice (Figure 5E). This defect could be due to either elevated lipid storage or elevated bile acids.

FXR regulation of gluconeogenesis. To explore the possibility of direct regulation of gluconeogenesis by FXR, we tested the effect of CA on hepatic expression of several key genes involved in gluconeogenesis in WT and *FXR*$^{-/-}$ mice. As expected, no FXR mRNA was detected in *FXR*$^{-/-}$ mice with a cDNA probe corresponding to the deleted last exon from the targeting construct (11), and SHP expression was markedly lower. Feeding a 1% CA diet for 5 days increased SHP expression in WT mice and strongly decreased CYP7A1 expression, as expected (4, 11, 24). Both responses were lost in *FXR*$^{-/-}$ mice, indicating that FXR-SHP–independent mechanisms for repression observed in some circumstances (5, 6) were not active over this time course. Dietary CA also decreased expression of multiple gluconeogenic genes in WT mice, including PGC-1α, PEPCK, and G-6-Pase, and this response was completely absent in *FXR*$^{-/-}$ mice (Figure 6A). Hepatocyte nuclear factor 4α (HNF-4α) expression showed a similar response to CA treatment, and its basal expression was modestly increased in *FXR*$^{-/-}$ mice compared with WT mice.

Interestingly, not all genes involved in gluconeogenesis were affected in the same fashion. Pyruvate carboxylase expression (Figure 6B) was unaffected by CA treatment in either the WT or *FXR*$^{-/-}$ mice, whereas forkhead transcription factor FOXO1 mRNA levels were decreased in the *FXR*$^{-/-}$ mice compared with WT in the presence and absence of CA. We also studied the effect of CA treatment on 2 rate-limiting enzyme genes involved in the glycolytic pathway, glucokinase and pyruvate kinase. Pyruvate kinase expression was higher in *FXR*$^{-/-}$ livers but was not affected by CA. Glucokinase transcripts were increased by CA feeding in both the WT and *FXR*$^{-/-}$ mice, suggesting this effect might be due to CA stimulation of signaling pathways independent of FXR.

We then investigated whether the suppressed gluconeogenic gene expression affected serum glucose levels. Indeed, CA feeding decreased fasting glucose by approximately 50% in WT mice but did not have a statistically significant effect in *FXR*$^{-/-}$ mice (Figure 6C). Consistent with previous results (25), CA feeding also reduced serum triglyceride levels in the WT mice but not the *FXR*$^{-/-}$ mice (Figure 6D).

The increased expression of SHP provides 1 potential mechanism for these FXR-dependent negative effects, as observed in the bile acid negative feedback regulation of CYP7A1 expression (4–6, 24). We tested this hypothesis by studying the effects of CA feeding on gluconeogenic gene expression in *SHP*$^{-/-}$ mice. On the chow diet, *SHP*$^{-/-}$ mice responded in a manner similar to *FXR*$^{-/-}$ mice, showing somewhat higher serum glucose in both fed (152 ± 13 versus 135 ± 9 mg/dl in WT) and fasted conditions (139 ± 15 versus 105 ± 12 mg/dl in WT) without significant changes in insulin. As observed in the *FXR*$^{-/-}$ mice, the *SHP*$^{-/-}$ mice also did not show repression of PEPCK, PGC-1α, or G-6-Pase expression in response to CA feeding (Figure 6E). On a chow diet, they exhibited modestly elevated serum glucose in both fasted and fed conditions (Figure 6F) without significant changes in insulin. However, they did not decrease serum glucose in response to dietary CA, suggesting that this effect of CA is mediated through the induction of SHP by FXR. Taken together, these results allow us to conclude that the previously identified pathways of bile acid feedback regulation by the FXR-SHP nuclear receptor cascade (4–6, 24) also target glucose metabolism.

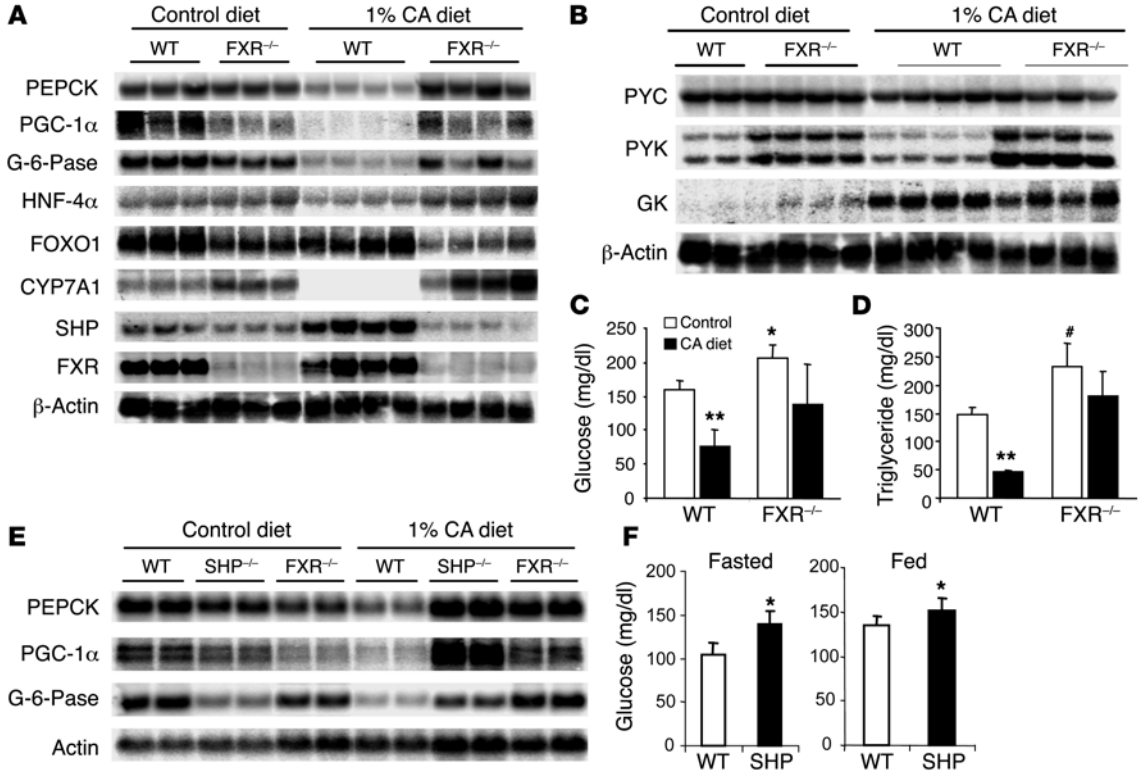

Figure 6

Effects of FXR agonists. Expression of genes involved in gluconeogenesis and glucose and triglyceride levels, which were measured after a 1% CA diet for 5 days. Glucose and triglyceride levels were measured at fed state from 6–7 mice per group and RNA from each group was pooled from 3–4 mice after overnight fasting. (**A**) Suppression of genes involved in gluconeogenesis by CA feeding was observed in WT but not *FXR*$^{-/-}$ mice. FOXO1, forkhead transcription factor FOXO1. (**B**) Effect of CA diet on glycolytic genes. GK, glucokinase; PYC, pyruvate carboxylase; PYK, pyruvate kinase. (**C**) Reduced serum glucose was observed in CA-fed WT mice. (**D**) Reduced triglyceride levels were seen in CA-fed WT mice. (**E**) SHP was required for suppressed expression of gluconeogenic genes in response to CA feeding. (**F**) Plasma glucose levels in fasted and fed WT and *SHP*$^{-/-}$ mice (n = 8 per group). $^{**}P < 0.01$ versus control diet; $^{*}P < 0.05$, $^{\#}P < 0.01$ versus WT.

Discussion

Our results provide 2 independent but complementary lines of evidence to show that the bile acid receptor FXR is a key regulator of glucose metabolism in vivo. As diagrammed in Figure 7, the first is that loss of FXR disrupts normal glucose homeostasis and leads to the development of insulin resistance as shown by hyperglycemia, impaired glucose tolerance, and severely blunted insulin signaling in both liver and muscle. This is associated with elevated serum triglycerides and lipid accumulation in *FXR*$^{-/-}$ livers, which has been ascribed to increased hepatic lipid production (12). The *FXR*$^{-/-}$ mice also showed markedly elevated circulating FFA levels comparable to those of WT mice on a high-fat diet, which is consistent with their elevated lipoprotein lipase activity (12). Second, FXR activation by CA suppressed expression of multiple genes involved in gluconeogenesis in WT mice but not *FXR*$^{-/-}$ or *SHP*$^{-/-}$ mice. This was associated with decreased fasting serum glucose in WT but not *FXR*$^{-/-}$ mice (Figure 6C), and preliminary results showed a similar effect in *SHP*$^{-/-}$ mice (our unpublished observations). These results indicate that the FXR-SHP negative regulatory cascade targets gluconeogenesis. Taken together, our results suggest that FXR function provides a novel molecular link between fatty liver and development of insulin resistance.

There are 2 major defects in glucose metabolism in *FXR*$^{-/-}$ mice: attenuated inhibition of glucose production in the liver in response to insulin and severely impaired peripheral glucose disposal. Both are the result of markedly blunted insulin signaling in these tissues associated with lipid accumulation. *FXR*$^{-/-}$ mice develop overt fatty liver, elevated levels of plasma FFAs, and elevated triglyceride and FFA levels in skeletal muscle.

In patients, the association of fat accumulation in the liver with insulin resistance is independent of obesity (13), and a recent study found that in nonobese, nondiabetic subjects fatty liver was both closely associated with and an early predictor of metabolic disorders such as hypertriglyceridemia and insulin resistance (14). Although the precise mechanisms linking fatty liver to diabetes remain unknown, the effect of elevated plasma FFAs on insulin sensitivity is well established. The contribution of elevated FFA to the development of peripheral insulin resistance was initially described in the Randle hypothesis (26), which suggested that higher FFA levels would compete with glucose for mitochondrial oxidation, leading to impaired glucose usage (27). More recently, a number of studies have revealed that FFAs interfere with the function of the insulin signaling pathway in skeletal muscle (28, 29), resulting in acquired insulin resistance. However, an intriguing recent study demonstrated that overexpression of PPARα in skeletal muscle results in insulin resistance via a distinct pathway associated with altered mitochondrial function (30). The apparent induction of expression of genes of fatty acid oxidation in the *FXR*$^{-/-}$ skeletal

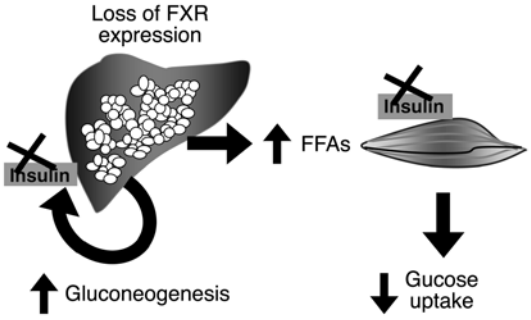

Figure 7
Dysregulation of hepatic and skeletal muscle glucose homeostasis in *FXR*$^{-/-}$ mice. Loss of FXR function in the liver results in increased hepatic lipid accumulation and elevation of FFAs in the serum. Insulin resistance both in the liver, which fails to suppress gluconeogenesis, and in the skeletal muscle, which reduces glucose uptake, contributes to dysregulation of glucose homeostasis in *FXR*$^{-/-}$ mice.

muscle is consistent with elevated PPARα activity. In addition, in an effort to rescue insulin resistance by lowering FFA levels, we treated mice with the PPARα agonists WY-14643 and fenofibrate. Instead of improving insulin sensitivity, both treatments further exacerbated the glucose intolerance in the *FXR*$^{-/-}$ mice (data not shown), suggesting that activation of the PPARα pathway in these animals is detrimental to insulin sensitivity. Thus we propose that the impaired insulin signaling in *FXR*$^{-/-}$ skeletal muscle is due to the adverse effects of elevated circulating FFA levels.

In the fed state, when insulin-dependent glucose uptake is the major determinant, *FXR*$^{-/-}$ mice show hyperglycemia that is consistent with their reduced peripheral insulin sensitivity. Peripheral insulin resistance in *FXR*$^{-/-}$ mice was confirmed by both the impaired glucose tolerance after glucose challenge and the decreased glucose disposal rate in the hyperinsulinemic clamp. However, blood glucose levels are dependent not only on peripheral glucose uptake, but also on glucose output from the liver. In human subjects, fat accumulation in the liver is associated with defects in insulin action in this tissue (13). Consistent with this, the livers of *FXR*$^{-/-}$ mice were also insulin resistant as shown by elevated fasting glucose levels in relatively older (3-month-old) animals, the failure to suppress glucose production in the low-dose clamp condition, and direct analysis of insulin signaling pathways. Interestingly, *FXR*$^{-/-}$ mice were also defective in the induction of gluconeogenic genes, including PGC-1α and PEPCK, after fasting (Figure 5E), which is consistent with a recent report of decreased expression of these genes in fasted *FXR*$^{-/-}$ livers (19). This failure to induce gluconeogenesis may contribute to the relative normalization of glucose levels in younger *FXR*$^{-/-}$ mice (Figure 1). The basis for this defect is not clear, but it could be a reflection of elevated FFA or other consequences of FXR deficiency in the liver, including elevated bile acid levels, which could affect the response of gluconeogenic genes to inductive signals such as glucocorticoids or cAMP. Taken together, we conclude that both peripheral and hepatic insulin resistance contribute to dysregulation of glucose homeostasis in *FXR*$^{-/-}$ mice (Figure 7). It is possible that either genetic or pharmacologic loss of FXR function could contribute to insulin resistance in patients with fatty liver disease.

If the absence of FXR leads to insulin resistance, does its activation promote insulin sensitivity? CA feeding in WT but not *FXR*$^{-/-}$ mice suppressed the expression of multiple genes in the gluconeogenic pathway, including PGC-1α, PEPCK, and G-6-Pase, and significantly lowered plasma glucose. These alterations in gluconeogenic gene expression were also lost in *SHP*$^{-/-}$ mice, strongly suggesting that they are dependent on the FXR-SHP negative regulatory pathway previously associated with negative feedback regulation of both bile acid (4–6, 24) and triglyceride (25) production. One recent study found that SHP represses the PEPCK and G-6-Pase promoters through its interaction with the glucocorticoid receptor (17), while another suggested that SHP could suppress these promoters through its interaction with a nonreceptor target, HNF-3 (31). Transgenic overexpression of SHP in the liver markedly decreases bile acid production via direct effects on CYP7A1 and other promoters, while effects on other pathways, including lipogenesis, appear indirect (32). Thus SHP activation may modulate gluconeogenesis via several mechanisms that remain to be elucidated.

These specific responses of gluconeogenic genes to activation of FXR contrast with their attenuated induction by fasting in the *FXR*$^{-/-}$ mice. Elevated bile acids activate FXR-independent signaling pathways such as JNK, PKC, and MAPK (20–22), and CA feeding had disparate effects on other genes, for example, inducing glucokinase expression in an FXR-independent manner. In accord with the decrease in hepatic glucose production predicted by the effects on gluconeogenic gene expression, the CA diet markedly lowered fasting glucose levels in the WT mice. These effects of CA mimic the response of the liver to feeding, raising the intriguing possibility that the return of reabsorbed bile acids to the liver, arriving with the co-absorbed nutrients, provides a signal that could function in concert with insulin and facilitate the energy switch occurring at the fasting-feeding transition.

In contrast to the results with CA feeding, we did not observe similar effects on gluconeogenic gene expression or glucose metabolism in several different treatments with the synthetic FXR agonist GW4064 over comparable time courses (data not shown). In these experiments, appropriate responses of SHP, CYP7A1, and other FXR targets at early time points confirmed the general effectiveness of the treatment, but these responses were blunted or absent as treatments continued (3–7 days). This indicates that the apparent lack of effect of GW4064 on glucose metabolism may be due to problems with the in vivo pharmacokinetics of this synthetic ligand. Alternatively, differences observed in effects of different FXR agonists (33) suggest that GW4064 may be a selective FXR modulator unable to activate a full response that encompasses the effects on glucose metabolism. However, it seems more likely that bile acid activation of additional signaling pathways (20–22) may be required to complement the FXR-dependent effects of CA on glucose metabolism.

The current results contrast with a recent report indicating that FXR agonists induced, rather than decreased, expression of PEPCK, but tended to increase plasma glucose (18). The authors' in vitro studies with chenodeoxycholic acid and GW4064 obviously differ from our in vivo studies, and their in vivo treatment protocols (50 mg/kg GW4064 i.p. twice daily) differed from ours (35 mg/kg oral gavage daily). Overall, however, our failure to observe a clear effect of GW4064 on glucose levels is consistent with these prior results (18).

In conclusion, we have demonstrated that FXR is required for the maintenance of glucose homeostasis in vivo. As observed in

type 2 diabetes, the altered glucose homeostasis in *FXR*$^{-/-}$ mice includes both dysregulated gluconeogenesis in liver and blunted insulin signaling in muscle. In addition, activation of FXR by CA suppresses gluconeogenic gene expression through the induction of SHP. *FXR*$^{-/-}$ mice provide what we believe to be a unique animal model that links fatty liver with development of insulin resistance and type 2 diabetes.

Methods

Animals. *FXR*$^{-/-}$ mice were obtained from F. Gonzalez (NIH, Bethesda, Maryland, USA) and backcrossed to C57BL/6J background for 5 generations. *SHP*$^{-/-}$ mice were generated previously in this laboratory (5) and backcrossed to C57BL/6J background for 5 generations. Genotyping of the mice was performed as described previously (5, 11). C57BL/6J WT mice were used as controls. Mice were maintained in the accredited pathogen-free Baylor College of Medicine Transgenic Mice Facility on a 12-hour light/dark cycle with free access to food and water. All experiments were done following approval of the protocol by the animal care research committee of Baylor College of Medicine.

Plasma glucose and lipids assays. Unless otherwise indicated, all plasma samples were drawn from mice at 8–12 weeks of age after overnight fasting. Glucose kits were purchased from Sigma-Aldrich (GPO-trinder), cholesterol and triglyceride kits were obtained from Thermo DMA Inc., and FFA acid kits were obtained from WAKO Chemicals Inc. Leptin was measured by ELISA (R&D Systems).

GTT and ITT. We performed i.p. GTTs and ITTs on 8- to 12-week-old mice. For GTTs, mice were injected a glucose dose of 2 g/kg of body weight after overnight fasting. For ITTs, random fed mice were injected with an insulin dose (Humulin R; Eli Lily and Co.) of 0.5 U/kg body weight and were fasted throughout the experiment. Insulin level was determined using a rat insulin ELISA kit (Crystal Chem Inc.).

Low-and high-dose hyperinsulinemic euglycemic clamp study. Mice were cannulated as described previously (34). Briefly, mice were anesthetized, and the right jugular vein was exposed via a midline neck incision through which a microcannula was inserted, threaded into the right atrium, and anchored at the venotomy site. Mice were allowed to recover for 4 days before the clamp. After an overnight fast, chronically catheterized conscious mice received a primed infusion (10 μCi) and then a constant rate intravenous infusion (0.1 μCi/min) of high pressure liquid chromatography–purified ^{3}H-glucose (PerkinElmer) using a syringe infusion pump (KD Scientific). For determination of basal glucose production, blood samples were collected from the tail vein after 50, 55, and 60 minutes of labeled glucose infusion. After 60 minutes, mice were primed with regular insulin (bolus 40 mU/kg body weight) followed by a 2-hour insulin infusion (3 mU/kg/min). Simultaneously, 10% glucose was infused using another infusion pump at a rate adjusted to maintain the blood glucose level at 100–140 mg/dl (low-dose hyperinsulinemic euglycemic clamp). Blood glucose concentration was determined every 10 minutes by a glucometer (LifeScan Inc.). Near the end of a 120-minute period (at 100, 110, and 120 min), blood was collected to measure hepatic glucose production and peripheral glucose disposal rates (35–37). A high-dose hyperinsulinemic euglycemic clamp was then started using 10 mU/kg/min insulin infusion and continued for 120 minutes to measure in vivo glucose utilization according to the method of Fujita et al. (35) with slight modifications. We monitored the plasma glucose level every 6–10 minutes. At the end of 120 minutes, blood was collected to measure the glucose disposal rate, and the total body glucose infusion rate was calculated.

Northern blotting analysis. Total RNA was isolated from snap-frozen liver or muscle tissues using Trizol reagent (Invitrogen Corp.). Northern blots were performed as previously described (34) using 20 μg total RNA fractionated on 1.2% 2 M formaldehyde agarose gels and transferred to Zeta-Probe GT genomic membrane (Bio-Rad). Gene-specific cDNA probes amplified by RT-PCR were used for hybridization in UltraHyb buffer (Ambion) at 42°C overnight. The FXR cDNA probe corresponded to the deleted last exon in the targeting construct of bp 1220–1698 of GeneBank cDNA NM009108.

Tissue triglyceride and FFA content analysis. Liver and muscle triglyceride and FFA content was analyzed using chloroform-methanol extraction and enzymatic assay kits (Thermo DMA Inc. and WAKO Chemicals Inc., respectively). Quadriceps was used for muscle analysis, and care was taken to avoid extracapsular fat tissues for this purpose. Total lipids were resuspended in 0.2% Triton-100 solution after extraction, followed by triglyceride assay using a kit from Thermo DMA Inc. and FFA assay using a kit from WAKO Pure Chemicals Industries Ltd.

IP and IB. For IP, 4 mg total protein was incubated with 4 μg of indicated antibodies at 4°C overnight, before incubation with protein A/G agarose beads at 4°C for 2 hours. After washing, beads were resuspended in Laemmli buffer before resolution by SDS-PAGE. Proteins were transferred to nitrocellulose membrane after electrophoresis and detected by chemiluminescence (Supersignal; Pierce Biotechnology). Monoclonal anti-phosphotyrosine antibody and polyclonal anti-PI3K P85 antibody were obtained from Upstate USA Inc. Rabbit polyclonal anti-IR antibody was a gift from Joslin Diabetes Center. Anti–phospho-Akt (Ser473) and anti–Akt-2 antibodies were obtained from Cell Signaling Technology.

In vivo insulin stimulation and analysis of insulin signaling. Mice were fasted overnight and injected i.p. with 5 U/kg body weight of regular insulin (Humulin; Eli Lilly and Company). Mice were sacrificed 5 minutes after insulin stimulation. Liver and muscle was removed, snap-frozen in liquid nitrogen, and stored at –80°C until use. Liver and muscle tissue were homogenized in protein lysis buffer containing 50 mM Tris-HCl, pH 7.4; 1% NP-40; 0.25% sodium deoxycholate; 150 mM NaCl; 1 mM EDTA; 1 mM PMSF; 1 μg/ml each of aprotinin, leupeptin, and pepstatin; 1 mM Na_3VO_4; and 1 mM NaF.

PI3K activity assay. PI3K activity was assayed in 4G10 anti-phosphotyrosine antibody IPs from muscle and liver extracts as previously described (38, 39). Extracted reaction products were resolved by thin-layer chromatography using Silica gel 60 plates (EMD Chemicals Inc.), and phosphorylated lipids were visualized by autoradiography.

Statistics. Values are expressed as mean ± SD. The differences between different genotypes were calculated by the 2-tailed Student's *t* test. $P < 0.05$ was considered statistically significant.

Note added in proof. After this work was completed, similar results were reported by Cariou et al. (40) and Zhang et al. (41).

Acknowledgments

Research was supported by NIH grants R01 DK53366 and U19 DK62434 (to D.D. Moore), American Heart Association Postdoctoral Fellowship AHA-0425117Y (Texas Affiliate; to K. Ma), and NIH grants R01 DK68037 and R01 HL-51586 (to L. Chan). We thank X-Ceptor Therapeutics Inc. for supplying GW4064, and Franck Mauvais-Jarvis for guidance on PI3K assays.

Received for publication May 10, 2005, and accepted in revised form January 31, 2006.

Address correspondence to: David D. Moore, Department of Molecular and Cellular Biology, Baylor College of Medicine, One Baylor Plaza, Houston, Texas 77030, USA. Phone: (713) 798-3313; Fax: (713) 798-3017; E-mail: moore@bcm.tmc.edu.

1. Parks, D.J., et al. 1999. Bile acids: natural ligands for an orphan nuclear receptor. *Science.* **284**:1365–1368.
2. Makishima, M., et al. 1999. Identification of a nuclear receptor for bile acids. *Science.* **284**:1362–1365.
3. Wang, H., Chen, J., Hollister, K., Sowers, L.C., and Forman, B.M. 1999. Endogenous bile acids are ligands for the nuclear receptor FXR/BAR. *Mol. Cell.* **3**:543–553.
4. Goodwin, B., et al. 2000. A regulatory cascade of the nuclear receptors FXR, SHP-1, and LRH-1 represses bile acid biosynthesis. *Mol. Cell.* **6**:517–526.
5. Wang, L., et al. 2002. Redundant pathways for negative feedback regulation of bile acid production. *Dev. Cell.* **2**:721–731.
6. Kerr, T.A., et al. 2002. Loss of nuclear receptor SHP impairs but does not eliminate negative feedback regulation of bile acid synthesis. *Dev. Cell.* **2**:713–720.
7. Holt, J.A., et al. 2003. Definition of a novel growth factor-dependent signal cascade for the suppression of bile acid biosynthesis. *Genes Dev.* **17**:1581–1591.
8. Urizar, N.L., Dowhan, D.H., and Moore, D.D. 2000. The farnesoid X-activated receptor mediates bile acid activation of phospholipid transfer protein gene expression. *J. Biol. Chem.* **275**:39313–39317.
9. Claudel, T., et al. 2003. Farnesoid X receptor agonists suppress hepatic apolipoprotein CIII expression. *Gastroenterology.* **125**:544–555.
10. Claudel, T., et al. 2002. Bile acid-activated nuclear receptor FXR suppresses apolipoprotein A-I transcription via a negative FXR response element. *J. Clin. Invest.* **109**:961–971. doi: 10.1172/JCI200214505.
11. Sinal, C.J., et al. 2000. Targeted disruption of the nuclear receptor FXR/BAR impairs bile acid and lipid homeostasis. *Cell.* **102**:731–744.
12. Lambert, G., et al. 2003. The farnesoid X-receptor is an essential regulator of cholesterol homeostasis. *J. Biol. Chem.* **278**:2563–2570.
13. Seppala-Lindroos, A., et al. 2002. Fat accumulation in the liver is associated with defects in insulin suppression of glucose production and serum free fatty acids independent of obesity in normal men. *J. Clin. Endocrinol. Metab.* **87**:3023–3028.
14. Kelley, D.E., McKolanis, T.M., Hegazi, R.A., Kuller, L.H., and Kalhan, S.C. 2003. Fatty liver in type 2 diabetes mellitus: relation to regional adiposity, fatty acids, and insulin resistance. *Am. J. Physiol. Endocrinol. Metab.* **285**:E906–E916.
15. De Fabiani, E., et al. 2003. Coordinated control of cholesterol catabolism to bile acids and of gluconeogenesis via a novel mechanism of transcription regulation linked to the fasted-to-fed cycle. *J. Biol. Chem.* **278**:39124–39132.
16. Duran-Sandoval, D., et al. 2004. Glucose regulates the expression of the farnesoid X receptor in liver. *Diabetes.* **53**:890–898.
17. Yamagata, K., et al. 2004. Bile acids regulate gluconeogenic gene expression via small heterodimer partner-mediated repression of hepatocyte nuclear factor 4 and Foxo1. *J. Biol. Chem.* **279**:23158–23165.
18. Stayrook, K.R., et al. 2005. Regulation of carbohydrate metabolism by the farnesoid X receptor. *Endocrinology.* **146**:984–991.
19. Cariou, B., et al. 2005. Transient impairment of the adaptive response to fasting in FXR-deficient mice. *FEBS Lett.* **579**:4076–4080.
20. Gupta, S., et al. 2004. Deoxycholic acid activates the c-Jun N-terminal kinase pathway via FAS receptor activation in primary hepatocytes. Role of acidic sphingomyelinase-mediated ceramide generation in FAS receptor activation. *J. Biol. Chem.* **279**:5821–5828.
21. Milkiewicz, P., Roma, M.G., Elias, E., and Coleman, R. 2002. Hepatoprotection with tauroursodeoxycholate and beta muricholate against taurolithocholate induced cholestasis: involvement of signal transduction pathways. *Gut.* **51**:113–119.
22. Fang, Y., et al. 2004. Bile acids induce mitochondrial ROS, which promote activation of receptor tyrosine kinases and signaling pathways in rat hepatocytes. *Hepatology.* **40**:961–971.
23. Le Marchand-Brustel, Y., et al. 2003. Fatty acid-induced insulin resistance: role of insulin receptor substrate 1 serine phosphorylation in the retroregulation of insulin signalling. *Biochem. Soc. Trans.* **31**:1152–1156.
24. Lu, T.T., et al. 2000. Molecular basis for feedback regulation of bile acid synthesis by nuclear receptors. *Mol. Cell.* **6**:507–515.
25. Watanabe, M., et al. 2004. Bile acids lower triglyceride levels via a pathway involving FXR, SHP, and SREBP-1c. *J. Clin. Invest.* **113**:1408–1418. doi:10.1172/JCI200421025.
26. Randle, P.J., Garland, P.B., Hales, C.N., and Newsholme, E.A. 1963. The glucose fatty-acid cycle. Its role in insulin sensitivity and the metabolic disturbances diabetes mellitus. *Lancet.* **1**:785–789.
27. Ruderman, N.B., Saha, A.K., Vavvas, D., and Witters, L.A. 1999. Malonyl-CoA, fuel sensing, and insulin resistance. *Am. J. Physiol.* **276**:E1–E18.
28. Shulman, G.I. 2000. Cellular mechanisms of insulin resistance. *J. Clin. Invest.* **106**:171–176.
29. Petersen, K.F., and Shulman, G.I. 2002. Pathogenesis of skeletal muscle insulin resistance in type 2 diabetes mellitus. *Am. J. Cardiol.* **90**:11G–18G.
30. Finck, B.N., et al. 2005. A potential link between muscle peroxisome proliferator-activated receptor-α signaling and obesity-related diabetes. *Cell Metab.* **1**:133–144.
31. Kim, J.Y., et al. 2004. Orphan nuclear receptor small heterodimer partner represses hepatocyte nuclear factor 3/Foxa transactivation via inhibition of its DNA binding. *Mol. Endocrinol.* **18**:2880–2894.
32. Boulias, K., et al. 2005. Regulation of hepatic metabolic pathways by the orphan nuclear receptor SHP. *EMBO J.* **24**:2624–2633.
33. Downes, M., et al. 2003. A chemical, genetic, and structural analysis of the nuclear bile acid receptor FXR. *Mol. Cell.* **11**:1079–1092.
34. Saha, P.K., Kojima, H., Martinez-Botas, J., Sunehag, A.L., and Chan, L. 2004. Metabolic adaptations in the absence of perilipin: increased beta-oxidation and decreased hepatic glucose production associated with peripheral insulin resistance but normal glucose tolerance in perilipin-null mice. *J. Biol. Chem.* **279**:35150–35158.
35. Fujita, Y., et al. 1998. Increased intestinal glucose absorption and postprandial hyperglycaemia at the early step of glucose intolerance in Otsuka Long-Evans Tokushima Fatty rats. *Diabetologia.* **41**:1459–1466.
36. Ma, K., et al. 2002. Increased beta-oxidation but no insulin resistance or glucose intolerance in mice lacking adiponectin. *J. Biol. Chem.* **277**:34658–34661.
37. Kim, J.K., Gavrilova, O., Chen, Y., Reitman, M.L., and Shulman, G.I. 2000. Mechanism of insulin resistance in A-ZIP/F-1 fatless mice. *J. Biol. Chem.* **275**:8456–8460.
38. Ueki, K., et al. 2000. Restored insulin-sensitivity in IRS-1-deficient mice treated by adenovirus-mediated gene therapy. *J. Clin. Invest.* **105**:1437–1445.
39. Mauvais-Jarvis, F., et al. 2002. Reduced expression of the murine p85α subunit of phosphoinositide 3-kinase improves insulin signaling and ameliorates diabetes. *J. Clin. Invest.* **109**:141–149. doi:10.1172/JCI200213305.
40. Cariou, B., et al. 2006. The farnesoid X receptor modulates adiposity and peripheral insulin sensitivity in mice. *J. Biol. Chem.* doi:10.1074/jbc.M510258200.
41. Zhang, Y., et al. 2006. Activation of the nuclear receptor FXR improves hyperglycemia and hyperlipidemia in diabetic mice. *Proc. Natl. Acad. Sci. U. S. A.* **103**:1006–1011.